Polar Geosci., 14, 88–98, 2001

Sm-Nd mineral isochron age of sapphirine-quartz gneiss from the Mt. Riiser-Larsen area in the Napier Complex, East Antarctica

Satoko Suzuki[1], Hiroo Kagami[1], Hideo Ishizuka[2] and Tomokazu Hokada[3,*]

[1]*Graduate School of Science and Technology, Niigata University, Ikarashi, Niigata 950-2181*
[2]*Department of Geology, Kochi University, Akebono-cho 2-chome, Kochi 780-8520*
[3]*National Institute of Polar Research, Kaga 1-chome, Itabashi-ku, Tokyo 173-8515*

Abstract: The Archaean Napier Complex in East Antarctica yields gneisses, including sapphirine+quartz assemblage that is diagnostic of ultra-high temperature (UHT) metamorphism. We determined an Sm-Nd mineral isochron age of the sapphirine-quartz gneiss from the Mt. Riiser-Larsen area for examining the timing of UHT metamorphism. The minerals analyzed here include sapphirine, orthopyroxene, sillimanite, quartz and feldspar, and the result defines approximately the mineral isochron of 2.2 Ga. This age is different from the ages of the other gneisses in the central part of the Mt. Riiser-Larsen area (approximately 2.4 Ga by Sm-Nd mineral isochron analyses). It is, therefore, suggested that the southwestern end of the Mt. Riiser-Larsen area, where the analyzed sapphirine-quartz gneiss was sampled, may have a different geological history from the gneisses of the central part, or may have been permeated with secondary fluid after the peak metamorphism.

key words: Sm-Nd mineral isochron age, sapphirine-quartz gneiss, UHT metamorphism, the Mt. Riiser-Larsen area, Napier Complex

1. Introduction

The Napier Complex in East Antarctica is mainly composed of ultra-high temperature (UHT) granulite facies gneisses characterized by such unique minerals or mineral assemblages as osumilite, inverted pigeonite, orthopyroxene+sillimanite+quartz, and sapphirine+quartz (Dallwitz, 1968; Ellis, 1980; Grew, 1980, 1982; Motoyoshi and Matsueda, 1984, 1987; Sandiford and Powell, 1988; Harley and Hensen, 1990; Motoyoshi *et al.*, 1990). The geochronological data of the Napier Complex have been obtained by Rb-Sr and Sm-Nd whole-rock or mineral isochron methods, the Pb-Pb whole-rock isochron method, the chemical Th-U-total Pb isochron method (CHIME) and the SHRIMP U-Pb method. Although these data indicate the complex to have been metamorphosed at the middle Archaean to the early Proterozoic, there are in detail three age clusters of *ca.* 3.8 Ga, 3.3 to 2.7 Ga, and 2.6 to 2.3 Ga (James and Black, 1981; Black *et al.*, 1983; Black and James, 1983; McCulloch and Black, 1984; Black *et al.*,

* Present address: Department of Geology, National Science Museum, 3-23-1 Hyakunin-cho, Shinjuku-ku, Tokyo 169-0073.

1986; Owada *et al.*, 1994; Harley and Black, 1997; Shiraishi *et al.*, 1997; Tainosho *et al.*, 1998; Asami *et al.*, 1998; Suzuki, 2000). There is, however, no study to determine the mineral isochron age of UHT metamorphism using the index minerals of UHT metamorphism. In this study, we determined an Sm-Nd mineral isochron age using sapphirine coexisting with quartz.

2. Field occurrence and sample description

The Mt. Riiser-Larsen area, the largest outcrop (5×12 km) in the Napier Complex, is located along the eastern coastline of Amundsen Bay. This area is underlain by various kinds of granulite facies metamorphic rocks (Fig. 1), which represent the highest temperature portion in the Napier Complex (Harley and Hensen 1990). Unmetamorphosed intrusive rocks (dolerite dikes) cut these metamorphic rocks. The chronological data of 3.0 to 2.8 Ga and 2.6 to 2.3 Ga obtained from the gneisses in the Mt. Riiser-Larsen area (compiled by Ishikawa *et al.*, 2000) mostly fit within the age clusters from the whole complex described in the previous section.

In this area, there are many shear zones with width of several centimeters to a few meters. The largest is called the Riiser-Larsen Main Shear Zone (R-LMSZ) (Ishizuka *et al.*, 1998; Ishikawa *et al.*, 2000). The R-LMSZ, which is located in the western part of the area (Fig. 1), strikes from north to south and dips near-vertically. In the studied area, this zone is bounded to the west by the western part, and to the east by the central part. The R-LMSZ consists of blocks of sheared gneisses derived from the surrounding metamorphic rocks such as orthopyroxene felsic gneiss or garnet felsic gneiss. Although the geological structure such as dips and strikes of foliation is not so different between the western and central parts in the area, the lithology is slightly different between the two parts; in the western part, magnetite-quartz gneiss occurs on a large-scale but there is no garnet gneiss. The retrograde reaction textures following sapphirine+quartz represent the cooling under the pressure conditions below 0.8 to 0.9 GPa (sapphirine+quartz → orthopyroxene+sillimanite) in the western part, but in the central part below 0.6 to 0.8 GPa (sapphirine+quartz → cordierite or garnet) (Hokada, 1999).

The analyzed sample is one of the quartzo-feldspathic gneisses (Ishikawa *et al.*, 2000), and includes sapphirine+quartz assemblage (hereafter, it is called sapphirine-quartz gneiss). The red star in Fig. 1 indicates the sample locality in the southwestern end of the Mt. Riiser-Larsen area. This quartzo-feldspathic gneiss is dominantly exposed, forming a layer of approximately 40 m width (Fig. 2A). The analyzed sample is the sapphirine-bearing layer of 10 cm width (sample no.: SS96122803B-1), in which there are further finer layers composed of white and dark green colored layers (Fig. 2B). The white layers are composed of quartz, plagioclase, alkali-feldspar, orthopyroxene, sapphirine and sillimanite with minor amount of osumilite, of which sillimanite usually coexists with orthopyroxene or quartz (Fig. 2C). The dark green colored layers contain relatively abundant anhedral sapphirine and orthopyroxene, of which orthopyroxene often shows the elongated form, and sapphirine usually contacts directly with orthopyroxene or quartz (Fig. 2D). Zircon and monazite are included in both layers. Monazite of approximately 0.2 mm in length often borders sapphirine or orthopyroxene.

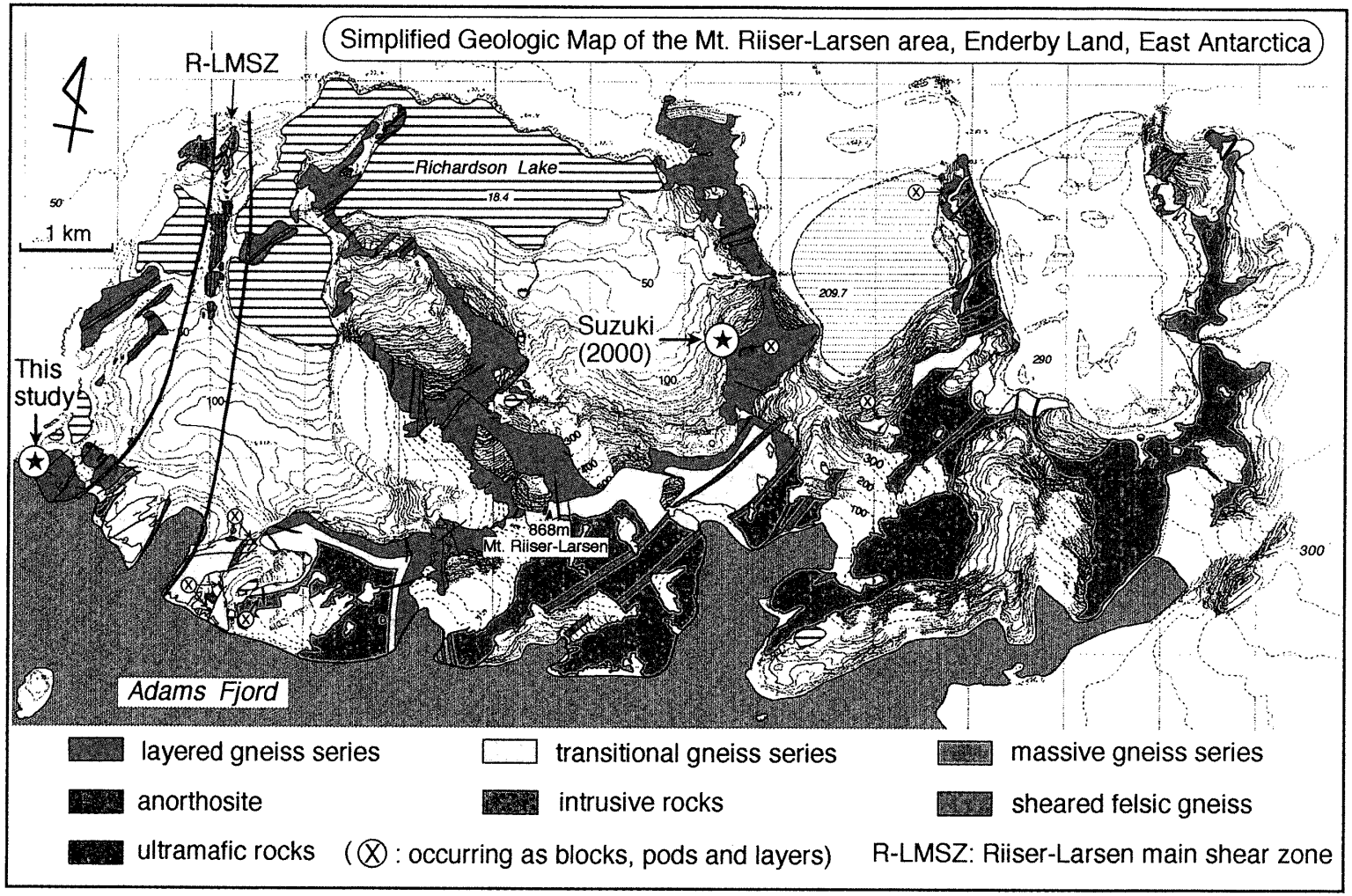

Fig. 1. The simplified geologic map of the Mt. Riiser-Larsen area (modified after Ishizuka et al., 1998). Red and blue stars indicate the sample localities of the analyzed sapphirine-quartz gneiss in the southwestern end (this study) and the other gneisses in the central part (Suzuki, 2000) of the Mt. Riiser-Larsen area, respectively.

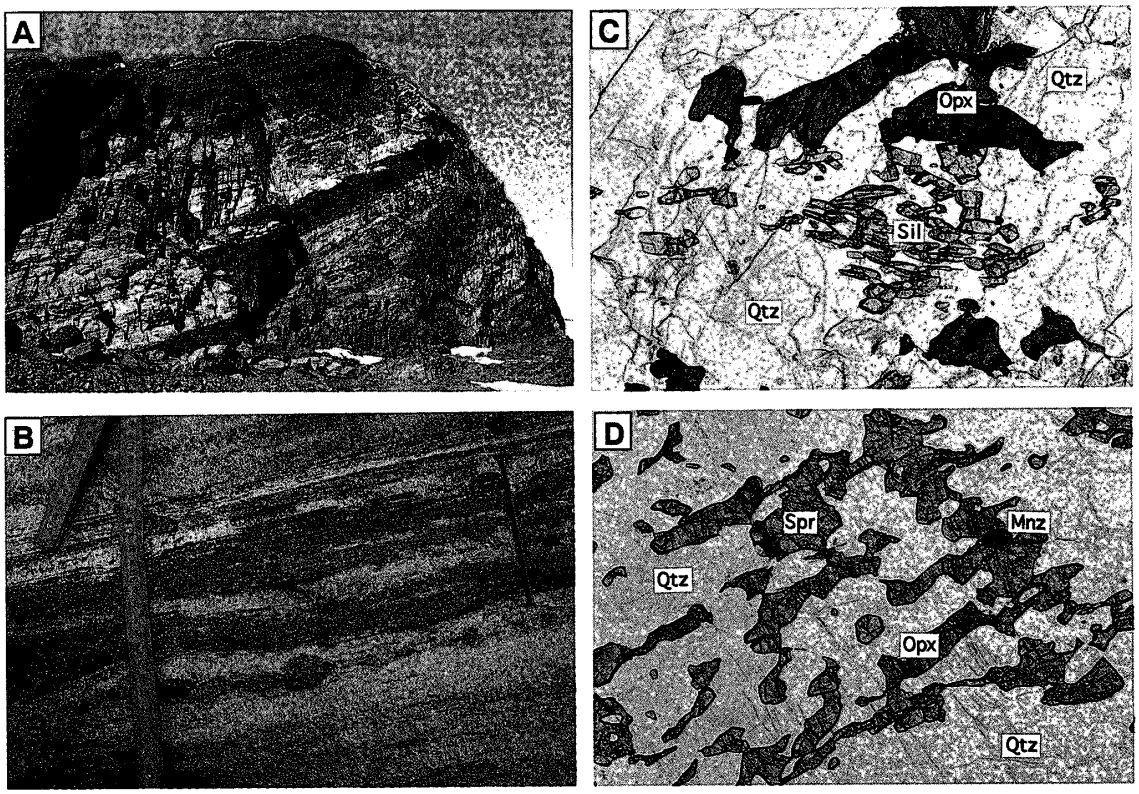

Fig. 2. (A) Outcrop of the analyzed sapphirine-quartz gneiss at the southwestern end of the Mt. Riiser-Larsen area. The width of the photograph is approximately 90 m. The red arrow points out the location of Fig. 2B. (B) Close-up view of Fig. 2A. The red bar indicates the analyzed layers. The white and dark green layers are mainly composed of quartz-plagioclase-alkali-feldspar and sapphirine-orthopyroxene, respectively. (C) Photomicrograph of the layer composed of orthopyroxene, sillimanite and quartz (width=2.5 mm). (D) Photomicrograph of sapphirine coexisting with quartz or orthopyroxene (width=2.5 mm). The abbreviations are as follows: Mnz: monazite; Opx: orthopyroxene, Qtz: quartz; Sil: sillimanite; Spr: sapphirine.

3. Analytical procedure

Mineral chemistries and whole-rock major and minor element compositions were obtained using EPMA (JEOL: JXA-8800) and X-ray fluorescence analyzer (XRF) (Rigaku: RIX-3000) at the National Institute of Polar Research, respectively. The rare earth elements (REE) of whole-rocks were analyzed with inductively coupled plasma mass spectrometry (ICP-MS) at Activation Laboratories Ltd. Sm and Nd isotopic composition analyses for whole-rocks and separated minerals were done by using the thermal ionization mass spectrometer (TIMS) (MAT-261 and 262) at the Graduate School of Science and Technology, Niigata University. Sm and Nd concentrations from the powdered samples were measured by the isotope dilution method with TIMS. The preparation and analytical method followed Yamamoto and Maruyama (1996) and Kagami *et al.* (1982, 1987). The $^{143}Nd/^{144}Nd$ ratio during the analyses was corrected to 0.512116 for JNdi-1 (GSJ standard). Sm-Nd concentration was measured using the ^{149}Sm-^{150}Nd mixed spike. Isochron ages were calculated using the personal computer program of Kawano (1994) based on the equation of York (1966) with the following

decay constant: λ (^{147}Sm)=6.54×10^{-12} y^{-1} (Lugmair and Marti, 1978).

4. Chemical compositions

4.1. Whole-rock composition

Table 1 shows the whole-rock composition of the analyzed sample. The sample has SiO_2 content of about 80 wt%, and Al_2O_3 content of about 10 wt%. Most important is the high MgO content of about 4 wt% for the SiO_2 content of about 80 wt%. Also, the Ni (55.9 ppm), Co (11.2 ppm) and Cr (27.2 ppm) contents are relatively high. These compositional features hardly indicate their precursor as igneous rocks, rather, they suggest the precursor to be a sedimentary rock mixed with minor basic to ultrabasic materials.

4.2. Mineral compositions

Table 1 shows the chemical compositions of representative minerals. Orthopyroxene grains were divided into two types (dark brown and light brown types), but these grains were mixed on isotope analyses because of their small amounts. In general, the grain size of the dark brown orthopyroxene is coarser than that of the light brown one. The Mg/(Mg+Fe) ratio of the dark brown orthopyroxene ranges from 0.72 to 0.75, while this ratio of light brown orthopyroxene ranges from 0.78 to 0.82, similar to those of co-existing sapphirine ranging from 0.77 to 0.85. This may be due to the difference of effective bulk composition in each orthopyroxene-bearing layer.

4.3. Isotope compositions

Table 2 shows the Sm and Nd concentrations and isotope compositions of whole-rock and mineral fractions. There are two aggregations of felsic fractions sampled from different white layers. Felsic fraction (FF)-1 is mainly composed of quartz and plagioclase, while felsic fraction (FF)-2 consists of quartz, plagioclase, alkali-feldspar and extremely minor sillimanite. Zircon and monazite in both felsic fractions cause the high Sm and Nd contents. The aggregations of sapphirine and orthopyroxene are high in purity for precise collecting by hand picking under a binocular microscope, although the orthopyroxene is a mixture of both dark brown one and light brown one. Sm and Nd concentrations of orthopyroxene and sapphirine are very low, 2.00 and 1.90 ppm, and 0.309 and 1.24 ppm, respectively. Thus the ^{143}Nd/^{144}Nd data of sapphirine is not good in accuracy because of its extremely low Nd concentration as well as its low modal proportion.

5. Results and interpretation

In this study, the Sm-Nd mineral isochron age using sapphirine of sapphirine-quartz gneiss was reported for the first time. The sample collected from the southwestern end of the Mt. Riiser-Larsen area was determined to be 2204±19 Ma (initial ^{143}Nd/^{144}Nd (NdI)=0.509250±0.000037) (Fig. 3). The geochronological data of the Napier Complex reported by previous authors make clusters of *ca.* 3.8 Ga, 3.3 to 2.7 Ga, and 2.6 to 2.3 Ga (Fig. 4). The age of 2.2 Ga is obviously younger than these age clusters.

Table 1. Mineral chemistries and whole-rock major and minor element compositions of the sapphirine-quartz gneiss.

sample	*Whole-rock*		
<XRF>		<ICP-MS>	
SiO_2 (wt.%)	80.87	Ga	14
TiO_2	0.15	Ge	0.7
Al_2O_3	9.69	La	27.9
Fe_2O_3	2.23	Ce	34
MnO	0.01	Pr	2.54
MgO	3.85	Nd	8.53
CaO	0.50	Sm	1.10
Na_2O	1.38	Eu	1.003
K_2O	0.39	Gd	0.80
P_2O_5	0.00	Tb	0.10
Total	99.06	Dy	0.42
FeO*	2.02	Ho	0.08
FeO*/MgO	0.53	Er	0.21
Ba (ppm)	977.8	Tm	0.024
Co	11.2	Yb	0.18
Cr	27.2	Lu	0.036
Cu	6.1	Hf	3.3
Nb	3.4	Ta	<0.1
Ni	55.9	Pb	17
Rb	5.7	Th	0.66
Sr	324.9	U	0.22
V	24.9		
Y	3.0		
Zn	33.5		
Zr	154.1		

mineral	*light brown orthopyroxene*			*dark brown orthopyroxene*		
SiO_2	49.85	50.23	49.20	48.18	49.64	50.10
TiO_2	0.02	0.18	0.41	0.15	0.10	0.17
Al_2O_3	12.04	11.16	11.83	11.50	10.66	10.10
Cr_2O_3	0.02	0.00	0.07	0.00	0.04	0.00
FeO	10.65	13.05	11.80	16.53	15.69	14.59
MnO	0.19	0.09	0.00	0.04	0.00	0.01
MgO	26.52	26.24	26.47	23.36	23.84	24.62
CaO	0.02	0.04	0.07	0.03	0.03	0.03
Na_2O	0.01	0.00	0.02	0.00	0.01	0.00
K_2O	0.00	0.00	0.00	0.00	0.00	0.00
Total	99.31	100.99	99.88	99.79	100.01	99.60
O	6	6	6	6	6	6
Si	1.763	1.767	1.742	1.745	1.783	1.798
Ti	0.000	0.005	0.011	0.004	0.003	0.005
Al	0.502	0.463	0.494	0.491	0.451	0.427
Cr	0.000	0.000	0.002	0.000	0.001	0.000
Fe	0.315	0.384	0.350	0.501	0.471	0.438
Mn	0.006	0.003	0.000	0.001	0.000	0.000
Mg	1.398	1.376	1.397	1.261	1.277	1.316
Ca	0.001	0.001	0.003	0.001	0.001	0.001
Na	0.000	0.000	0.002	0.000	0.001	0.000
K	0.000	0.000	0.000	0.000	0.000	0.000
Total cation	3.985	3.998	4.000	4.005	3.988	3.984
XAl	0.25	0.23	0.25	0.25	0.23	0.21
XMg	0.82	0.78	0.80	0.72	0.73	0.75

total Fe as FeO

Table 1. Continued.

mineral	*sapphirine*		
SiO_2	13.77	13.84	14.00
TiO_2	0.00	0.11	0.00
Al_2O_3	61.06	60.33	61.91
Cr_2O_3	0.00	0.03	0.04
FeO	9.23	9.23	6.20
MnO	0.00	0.03	0.06
MgO	15.85	16.35	17.67
CaO	0.00	0.01	0.02
Na_2O	0.03	0.02	0.01
K_2O	0.00	0.00	0.00
Total	99.93	99.95	99.91
O	10	10	10
Si	0.825	0.830	0.828
Ti	0.000	0.005	0.000
Al	4.313	4.266	4.315
Cr	0.000	0.001	0.002
Fe	0.463	0.463	0.307
Mn	0.000	0.002	0.003
Mg	1.416	1.462	1.557
Ca	0.000	0.001	0.001
Na	0.003	0.002	0.002
K	0.000	0.000	0.000
Total cation	7.020	7.032	7.014
XMg	0.75	0.76	0.84

total Fe as FeO

mineral	*sillimanite*	
SiO_2	37.07	37.23
TiO_2	0.00	0.02
Al_2O_3	61.99	61.53
Fe_2O_3	0.35	0.43
Cr_2O_3	0.00	0.00
MnO	0.00	0.00
MgO	0.01	0.02
CaO	0.03	0.00
Na_2O	0.00	0.01
K_2O	0.00	0.00
Total	99.45	99.25
O	5	5
Si	4.025	4.050
Ti	0.000	0.002
Al	7.935	7.892
Fe^{3+}	0.029	0.036
Cr	0.000	0.000
Mn	0.000	0.000
Mg	0.001	0.003
Ca	0.003	0.000
Na	0.001	0.003
K	0.000	0.000
Total cation	11.994	11.986

total Fe as Fe_2O_3

mineral	*feldspar*			
SiO_2	67.88	66.59	66.98	62.27
TiO_2	0.02	0.05	0.10	0.08
Al_2O_3	21.17	20.58	21.26	20.48
Fe_2O_3	0.06	0.08	0.08	0.02
Cr_2O_3	0.00	0.02	0.00	0.00
MnO	0.00	0.00	0.00	0.00
MgO	0.01	0.01	0.01	0.02
CaO	2.49	2.45	2.62	1.95
Na_2O	9.04	9.02	8.83	4.37
K_2O	0.23	0.25	0.32	8.38
BaO	0.06	0.00	0.00	1.11
Total	100.94	99.05	100.20	98.68
O	8	8	8	8
Si	2.937	2.938	2.922	2.879
Ti	0.000	0.002	0.003	0.003
Al	1.080	1.070	1.093	1.116
Fe^{3+}	0.002	0.002	0.002	0.001
Cr	0.000	0.001	0.000	0.000
Mn	0.000	0.000	0.000	0.000
Mg	0.000	0.001	0.001	0.002
Ca	0.115	0.116	0.122	0.096
Na	0.758	0.772	0.747	0.392
K	0.013	0.014	0.018	0.494
Ba	0.001	0.000	0.000	0.020
Total cation	4.907	4.916	4.909	5.003
an	0.130	0.129	0.138	0.098
ab	0.855	0.856	0.842	0.399
or	0.015	0.015	0.020	0.503

total Fe as Fe_2O_3

Table 2. Sm and Nd concentrations and isotope compositions of the sapphirine-quartz gneiss and its mineral fractions.

mineral	Sm (ppm)	Nd (ppm)	$^{147}Sm/^{144}Nd$	$^{143}Nd/^{144}Nd$	(2σ)
felsic fraction-1	9.28	69.8	0.08038	0.510396	(14)
felsic fraction-2	11.7	88.7	0.07979	0.510384	(11)
whole rock	6.90	50.4	0.08272	0.510464	(23)
orthopyroxene	2.00	1.90	0.6393	0.518528	(13)
sapphirine	0.309	1.24	0.1510	0.51148	(20)

Numbers in parentheses represent analytical reproducibility in terms of 2σ, referring to the last digits.

Furthermore, the other Sm-Nd mineral isochron ages of granitic orthogneiss, mafic granulite and paragneiss in the central part of the Mt. Riiser-Larsen area were restricted to ages of 2.36 to 2.38 Ga (Suzuki, 2000); the localities of these samples are indicated by a blue star in Fig. 1.

This difference may be caused by two possibilities: 1) the R-LMSZ is a significant tectonic boundary and the two parts against the R-LMSZ have different thermal history, or 2) influence of fluid permeated through the structure such as foliation, folding, shearing or jointing simultaneously with or after the peak metamorphism in the western part. In case 1), if all of the Sm-Nd mineral isochron data indicate the cooling age through the closure temperature for constituent minerals, the age difference between the central and the western parts may be caused by the difference of geological history between the two parts. Namely, the final timing to obtain a closed system (of Sm-Nd isotope systematics) in the western part may have been 200 m.y. after that in the central part. If it is not the case, gneisses of the western part may have suffered another UHT metamorphism at 2.2 Ga, which has not influenced the central part. These considerations are not in conflict with the estimate of pressure condition of retrograde metamorphism in

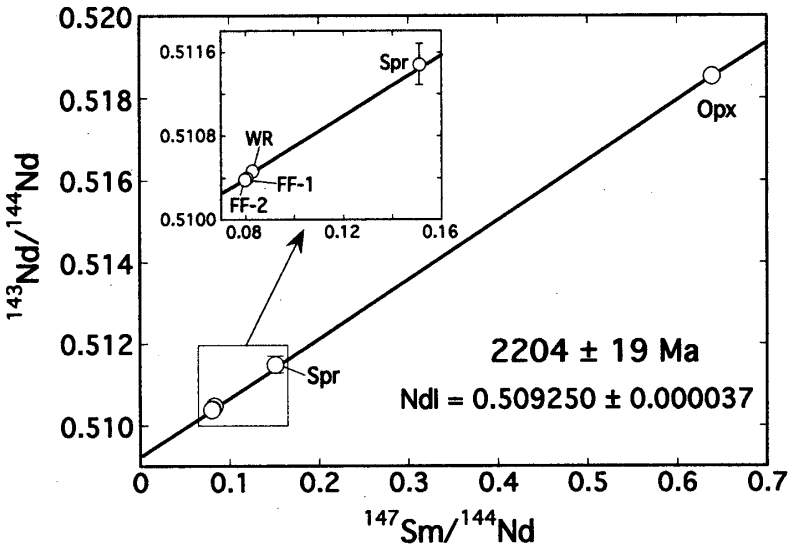

Fig. 3. Sm-Nd mineral isochron diagram for sapphirine-quartz gneiss from the Mt. Riiser-Larsen area. The abbreviations are as follows: FF: felsic fraction, WR: whole-rock, Spr: sapphirine, Opx: orthopyroxene mixture of the dark and light brown types. NdI: initial $^{143}Nd/^{144}Nd$.

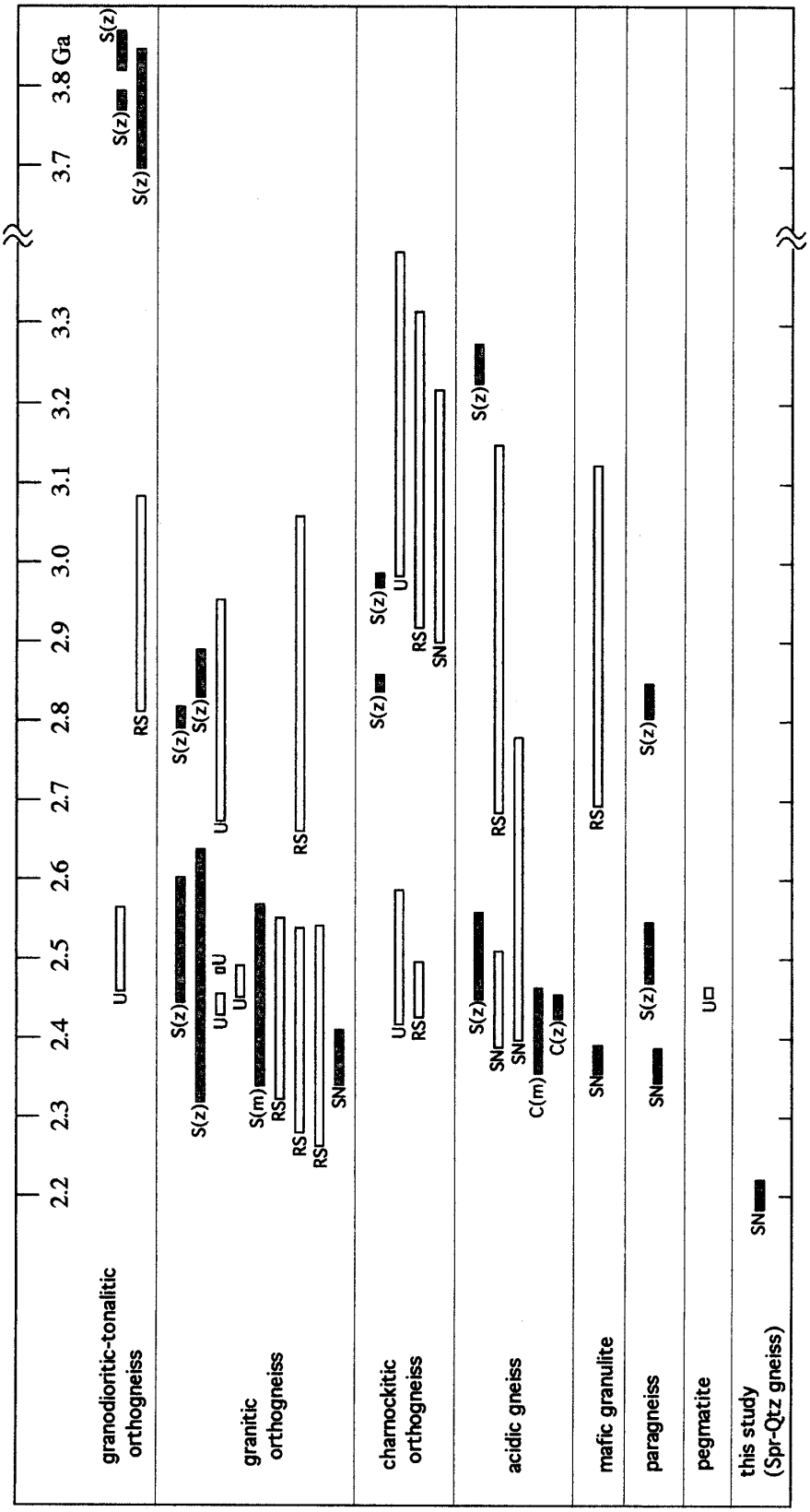

Fig. 4. Comparison of radiometric ages from the Napier Complex. Open and solid bars show the whole-rock and mineral ages, respectively. Lengths of bars represent error limits; in this figure, only the data with the errors smaller than ±500 m.y. are used. Capital letters indicate the dating methods such as SN=Sm-Nd, RS=Rb-Sr and U=U-Pb. SHRIMP U-Pb and CHIME U-Pb-Th ages are shown as S and C, respectively. The small letters z and m in parentheses represent zircon and monazite, respectively. Data sources are James and Black (1981), Black et al. (1983), Black and James (1983), McCulloch and Black (1984), Black et al. (1986), Owada et al. (1994), Harley and Black (1997), Shiraishi et al. (1997), Tainosho et al. (1998), Asami et al. (1998), and Suzuki (2000).

each part, suggesting the different thermal history of both parts (Hokada, 1999).

In case 2), it has been known that REE are extremely mobile in CO_2-rich solutions (Wendlandt and Harrison 1979). The sapphirine-quartz gneiss, cropping out in the western part, has been more or less sheared and cracked. If the primary fluid, including the CO_2 component, was present at the stage of the peak metamorphism, it may be useful for examining the timing of UHT metamorphism on Sm-Nd systematics. However, if the secondary fluid, including the CO_2 component, has permeated through a shear or crack after the peak metamorphism, the Sm-Nd mineral isochron age may record the final event or the mixing data (pseudo-isochron age) in the system (Touret, 2001).

We cannot now decide whether the calculated age depends on geological evolution or the secondary fluid activity. To examine this, we should compare the present result with the Sm-Nd mineral isochron age of the sapphirine-quartz gneiss from the central part.

Acknowledgments

We would like to express our thanks to Prof. K. Shiraishi, Dr. M. Owada and Mr. T. Miyamoto for their critical reading and useful comments. Thanks also go to Dr. T. Sakumoto and Ms M. Mori for their encouragement. NIPR is thanked for EPMA and XRF measurements, and JSPS is also appreciated for financial support during this study.

References

Asami, M., Suzuki, K., Grew, E.S. and Adachi, M. (1998): CHIME ages for granulites from the Napier Complex, East Antarctica. Polar Geosci., **11**, 172–199.

Black, L.P. and James, P.R. (1983): Geological history of the Napier Complex of Enderby Land. Antarctic Earth Science, ed. by R.L. Oliver *et al.* Canberra, Aust. Acad. Sci., 11–15.

Black, L.P., James, P.R. and Harley, S.L. (1983): Geochronology and geological evolution of metamorphic rocks in the Field Islands area, East Antarctica. J. Metamorph. Geol., **1**, 277–303.

Black, L.P., Sheraton, J.W. and James, P.R. (1986): Late Archaean granites of the Napier Complex, Enderby Land, Antarctica: A comparison of Rb-Sr, Sm-Nd and U-Pb isotopic systematics in a complex terrain. Precambrian Res., **32**, 343–368.

Dallwitz, W.B. (1968): Coexisting sapphirine and quartz in granulite from Enderby Land, Antarctica. Nature, **219**, 476–477.

Ellis, D.J. (1980): Osumilite-sapphirine-quartz granulites from Enderby Land, Antarctica: *P-T* conditions of metamorphism, implications for garnet-cordierite equilibria and the evolution of the deep crust. Contrib. Mineral. Petrol., **74**, 201–210.

Grew, E.S. (1980): Sapphirine-quartz association from Archean rocks in Enderby Land, Antarctica. Am. Mineral., **65**, 821–836.

Grew, E.S. (1982): Osumilite in the sapphirine-quartz terrane of Enderby Land, Antarctica: implications for osumilite petrogenesis in the granulite facies. Am. Mineral., **67**, 762–787.

Harley, S.L. and Black, L.P. (1997): A revised Archaean chronology for the Napier Complex, Enderby Land, from SHRIMP ion-microprobe studies. Antarct. Sci., **9**, 74–91.

Harley, S.L. and Hensen, B.J. (1990): Archaean and Proterozoic high-grade terranes of East Antarctica (40–80°): a case study of diversity in granulite facies metamorphism. High-temperature Metamorphism and Crustal Anatexis, ed. by J.R. Ashwoeth and M. Brouwn. London, Unwin Hyman, 320–370.

Hokada, T. (1999): Thermal evolution of the ultrahigh-temperature metamorphic rocks in the Archaean Napier Complex, East Antarctica. Ph.D. Thesis, The Graduate University for Advanced Studies, 126 p.

Ishikawa, M., Hokada, T., Ishizuka, H., Miura, M., Suzuki, S., Takada, M. and Zwartz, D.P. (2000): Explanatory text of geological map of Mount Riiser-Larsen, Enderby Land, Antarctica.

Antarctic geological map series sheet 37: Mount Riiser-Larsen. Tokyo, National Institute of Polar Research, 23 p.

Ishizuka, H., Ishikawa, M., Hokada, T. and Suzuki, S. (1998): Geology of the Mt. Riiser-Larsen area of the Napier Complex, Enderby Land, East Antarctica. Polar Geosci., **11**, 154–171.

James, P.R. and Black, L.P. (1981): A review of the structural evolution and geochronology of the Archaean Napier Complex of Enderby Land, Australian Antarctic Territory. Archaean Geology, ed. by J.E. Glover and D.I. Groves. Sydney, Geological Society of Australia, 71–83 (Special Publications, No. 7).

Kagami, H., Okano, O., Sudo, H. and Honma, H. (1982): Isotopic analysis of Rb and Sr using a full automatic thermal ionization mass spectrometer. Pap. Inst. Therm. Spring Res., Okayama Univ., **52**, 51–70.

Kagami, H., Iwata, M., Sano, S. and Honma, H. (1987): Sr and Nd isotopic compositions and Rb, Sr, Sm and Nd concentrations of standard samples. Tech. Rep. Inst. Study Earth's Inter., Okayama Univ., **B4**, 1–16.

Kawano, Y. (1994): Calculation program for isochron ages of Rb-Sr and Sm-Nd systems using personal computer. Geoinformatics, **5**, 13–19 (in Japanese with English abstract).

Lugmair, G.W. and Marti, K. (1978): Lunar initial $^{143}Nd/^{144}Nd$: differential evolution of the lunar crust and mantle. Earth Planet. Sci. Lett., **39**, 349–357.

McCulloch, M.T. and Black, L.P. (1984): Sm-Nd isotopic systematics of Enderby Land granulites and evidence for the redistribution of Sm and Nd during metamorphism. Earth Planet. Sci. Lett., **71**, 46–58.

Motoyoshi, Y. and Matsueda, H. (1984): Archean granulites from Mt. Riiser-Larsen in Enderby Land, East Antarctica. Mem. Natl Inst. Polar Res., Spec. Issue, **33**, 103–125.

Motoyoshi, Y. and Matsueda, H. (1987): Corundum+quartz association in Archean granulite-facies rock from Enderby Land, East Antarctica: preliminary interpretation. Proc. NIPR Symp. Antarct. Geosci., **1**, 107–112.

Motoyoshi, Y., Hensen, B.J. and Matsueda, H. (1990): Metastable growth of corundum adjacent to quartz in a spinel-bearing quartzite from the Archaean Napier Complex, Antarctica. J. Metamorph. Geol., **8**, 125–130.

Owada, M., Osanai, Y. and Kagami, H. (1994): Isotopic equilibration age of Sm-Nd whole-rock system in the Napier Complex (Tonagh Island), East Antarctica. Proc. NIPR Symp. Antarct. Geosci., **7**, 122–132.

Sandiford, M. and Powell, R. (1988): Pyroxene exsolution in granulites from Fyfe Hills, Enderby Land, Antarctica: evidence for 1000°C metamorphic temperatures in Archean continental crust. Am. Mineral., **73**, 434–438.

Shiraishi, K., Ellis, D.J., Fanning, C.M., Hiroi, Y. and Motoyoshi, Y. (1997): Re-examination of the metamorphic and protolith ages of the Rayner Complex, Antarctica: evidence for the Cambrian (Pan-African) regional metamorphic event. The Antarctic Region: Geological Evolution and Processes, ed. by C.A. Rocci. Siena, Terra Antarct. Publ., 79–88.

Suzuki, S. (2000): Geochemistry and geochronology of ultra-high temperature metamorphic rocks from the Mt. Riiser-Larsen area in the Archaean Napier Complex, East Antarctica. Ph.D. Thesis, The Graduate University for Advanced Studies, 109 p.

Tainosho, Y., Kagami, H., Hamamoto, T. and Takahashi, Y. (1998): Sm-Nd and Rb-Sr whole-rock systems of metamorphic rocks from Mount Pardoe in the Napier Complex, East Antarctica. Precambrian Crustal Processes in East Coast Granulite–Greenstone Regions of India and Antarctica within East Gondwana, ed. by A.T. Rao *et al.* Gondwana Res. Group Mem., **4**, 185-198.

Touret, J.L.R. (2001): Fluids in metamorphic rocks. Lithos, **55**, 1–25.

Wendlandt, R.F. and Harrison, W.J. (1979): Rare earth partitioning between immiscible carbonate and silicate liquids and CO_2 vapor: Results and implications for the formation of light rare earth-enriched rocks. Contrib. Mineral. Petrol., **69**, 409–419.

Yamamoto, M. and Maruyama, T. (1996): The Sr and Nd isotopic analysis and the quantitative analysis of Rb and Sr by using MAT 261. Tech. Rep. Inst. Appl. Earth Sci., Min. Eng. Mater. Process., Min. Coll., Akita Univ., **61**, 17–30.

York, D. (1966): Least-squares fitting of a straight line. Can. J. Phys., **44**, 1079–1086.

(Received March 21, 2001; Revised manuscript accepted May 30, 2001)